

# Hydrodynamic Flow from Fast Particles

J. Casalderrey-Solana, E. V. Shuryak, D. Teaney

*Department of Physics & Astronomy,  
SUNY at Stony Brook, Stony Brook, NY 11764, USA*

(Dated: August 30, 2018)

## Abstract

We study the interaction of a fast moving particle in the Quark Gluon Plasma with linearized hydrodynamics. We derive the linearized hydrodynamic equations on top of an expanding fireball, and detail the solutions for a static medium. There are two modes far from the jet – a sound mode and a diffusion mode. The diffusion mode is localized in a narrow wake behind the jet while the sound mode propagates at the Mach angle,  $\cos(\theta_M) = c_s/c$ . A general argument shows that the strength of the diffusion mode relative to the sound mode is directly proportional to the entropy produced by the jet-medium interaction. This argument does not rely on the linearized approximation and the assumption of local thermal equilibrium close to the jet. With this insight we calculate the spectrum of secondaries associated with the fast moving particle. If the energy loss is large and the jet-medium interaction does not produce significant entropy, the flow at the Mach angle can be observed in the associated spectrum. However, the shape of associated spectra is quite fragile and sensitive to many of the inputs of the calculation.

## I. INTRODUCTION

One of the major findings at RHIC is jet quenching, the suppression of high transverse momentum particles [1]. This strong suppression is attributed to the energy loss of partons traversing the dense medium formed in a high energy heavy ion collision. Different microscopic mechanisms for the jet energy loss have been proposed [2, 3, 4, 5, 6] (see Ref. [7] for a review).

Ultimately the energy “lost” by these fast partons is shared among the constituents of the medium. In a previous paper we argued that the fate of the deposited energy and momentum should be described by hydrodynamics<sup>1</sup> [8]. Hydrodynamic models describe the RHIC data reasonably well and motivated this suggestion. The suggestion was also motivated by the experimental observation of particles associated with a high  $p_T$  trigger at a particular azimuthal angle,  $\Delta\phi = \pi - 1.2$  rad, relative to the trigger particle [14, 15]. Within linearized hydrodynamics, jets induce flow fields with a conical shape similar to the supersonic flow past planes. It was argued that this conical flow could provide an explanation for the observed correlation. Discussion of alternative explanations to the large  $p_T$  correlations at RHIC can be found in Refs. [16, 17, 18, 19].

In this first paper we solved linearized hydrodynamics in a static homogeneous medium, and found that two modes can be excited – a sound mode and diffusion mode [8]. The relative strength of these modes depends on the jet-medium interaction and will be clarified in this work. Subsequently, the effect of the fireball expansion was studied [20], and an attempt to incorporate more realistic mediums has been made [21]. Further, the nonlinear hydrodynamic response to the jet was estimated with 2+1 dimensional hydro code [22]. The conical flow was not observed in the azimuthal correlations of that work; possible reasons for this are discussed in section VII. Finally, a parton transport calculation based on the AMPT model also found large angle di-hadron correlations [23, 24].

In a second paper two of us studied the conical flow in an expanding fireball with a variable speed of sound and found that the amplitude of the sound wave increases [25]. Furthermore, we have shown that a first order phase transition with a vanishing speed of sound, would lead to more peaks in the di-hadron correlation function. These additional peaks have not been observed.

In this paper we present a systematic study of the conical flow within the linearized theory. In section II we start by providing an overview and explaining the approximations. Then in section III, we review our calculation for a static medium and find the two modes of linearized hydrodynamics [8]. In section IV, we describe potential flow, first for an ideal fluid, and then with viscosity. Section IV also provides the linearized equations which propagate small perturbations over a general hydrodynamical expansion. In section V, we relate the energy and momentum loss of the jet to the outgoing sound waves at large distances. This result ties the initial energy loss to the normalization of the final spectrum of secondaries that is calculated in section VIII. Our work in section V also delineates two microscopic models for the jet-medium interaction based on entropy production. These two models are described in sections VI and VII, and their corresponding correlation functions are calculated in section VIII. Finally, many technical derivations are delegated into appendices.

---

<sup>1</sup> see Ref. [9] for a similar idea by Stocker.

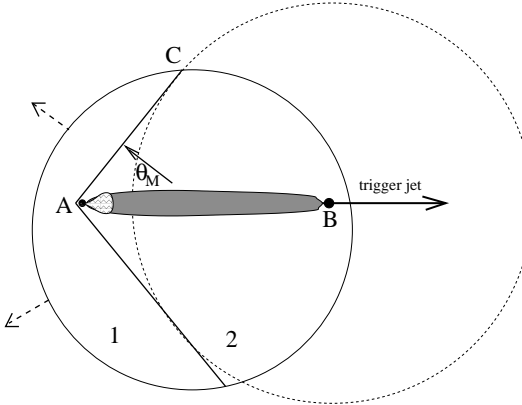


FIG. 1: A schematic picture of the flow created by a jet moving through the fireball. The trigger jet is moving to the right away from the origination point (the black circle at point B). Sound waves start propagating as spherical waves (the dashed circle) from the origination point. The companion quenched jet is moving to the left creating a wake of matter (shaded area) and adding to the sound wave. The head of the jet is a non-equilibrium gluonic shower formed by the original hard parton (black dot A). The solid arrow indicates the flow velocity which is perpendicular to the shock cone at the angle  $\theta_M$ ,  $\cos(\theta_M) = c_s/c \simeq 0.55$ .

## II. OVERVIEW

A schematic picture of di-jet production in a nucleus-nucleus collision is given in Fig. 1. For simplicity we will only consider a di-jet pair with both particles at mid-rapidity in a central Au-Au collision. One jet serves as the trigger particle and is biased toward the edge of the nucleus due to the strong jet quenching. The other jet then travels a distance  $2R_{\text{Au}} \sim 10 \text{ fm}$  and is either completely or partly absorbed. Experimentally a companion jet with  $p_T \sim 10 \text{ GeV}$  seems to be absorbed while a jet with larger transverse momentum seems to “punch through” and re-appear at an angle  $\Delta\phi = \pi$  relative to the trigger jet.

In general the rapidity of the two jets are not identical and this will complicate the experimental interpretation of our results. The particular configuration we are considering can be selected with three particle correlations and currently there is an experimental effort in this direction.

Far from the jet we can calculate the correlation of  $T^{\mu\nu}$  with the passage of the jet using linearized hydrodynamics. Generally there are two modes – a sound mode and a diffusion mode. The diffusion mode is concentrated in a narrow wake behind the jet while the sound mode propagates forward at the Mach angle,  $\cos(\theta_M) = c_s/c \simeq 0.55$ . The total momentum loss can be related to the amplitude of the wake and the amplitude of the sound wave. Under the reasonable assumption that the total energy and momentum loss of the jet are equal we reach the stronger conclusion which relates the entropy production of the jet to the relative strength of the two modes.

The equations for the sound wave are given by Eqs. (4.2), and (5.3). The unknown function in this formula,  $dF/dx$ , is related to the momentum transferred to the sound wave – see Eq. (6.5). Similarly the flow fields in the wake are given by Eq. (5.4), and the amplitude  $A$  in this formula is fixed by the momentum transferred to the wake – see Eq. (5.13). This momentum transfer is in turn related by Eq. (5.14) to the total entropy produced by the

jet. In summary, by specifying the total rate of energy loss and entropy production the flow fields at large distances are determined.

We next estimate the medium modifications at the head of the jet where the jet loses energy through collisional and radiative processes. Since the jet energy is large compared to the typical scale of the medium, the jet acts as a point source. The energy deposited by this source is distributed into the surrounding fluid through highly dissipative processes. To estimate the order of magnitude of the initial modification, consider a jet that losses certain amount of energy per unit length,  $dE/dx$ . This energy is absorbed by the medium over a dissipative length scale of the order of the sound attenuation length,  $\Gamma_s = 4\eta/3w$ , where  $\eta$  is the shear viscosity and  $w = e + p$  is enthalpy of the medium. Thus we compare the energy deposited by the jet in this typical length  $\Gamma_s$  with the energy of the fluid in a deposition volume of  $\Gamma_s^3$ ,

$$\frac{E_{\text{lost}}}{E_{\text{fluid}}} \approx \frac{\frac{dE}{dx} \times \Gamma_s}{e \times \Gamma_s^3}. \quad (2.1)$$

To estimate this initial modification, we use the formula from Ref. [5] for radiative energy loss

$$-\frac{dE}{dx} = \frac{\alpha_s C_R}{8} \frac{\mu^2}{\lambda_g} L \ln \frac{L}{\lambda_g}, \quad (2.2)$$

where  $\frac{\mu^2}{\lambda_g} = \hat{q}$  is the transport coefficient. Perturbative estimates for this parameter give  $\hat{q} = 0.6 \text{ GeV}^2/\text{fm}$  for  $T = 200 \text{ MeV}$  [26]. Setting  $\lambda_g \approx 1 \text{ fm}$  [26],  $L = 5 \text{ fm}$ , and  $C_R = 3$  (gluons), we obtain,  $dE/dx \approx 2.7 \text{ GeV/fm}$ . Similarly, perturbative estimates for the sound attenuation length give with  $\alpha_s = 1/2$ ,  $\Gamma_s \approx 0.18/T$  [11, 12]. The conjectured lower bound for  $\Gamma_s$  is  $1/3\pi T$  [28]. For the energy density of the unperturbed medium ( $e$ ) we will take the QGP value as measured on the lattice,  $e \approx 12T^4$  [27]. For  $T = 200 \text{ MeV}$ , we finally conclude that

$$\frac{E_{\text{lost}}}{E_{\text{fluid}}} \approx \frac{\frac{dE}{dx} \times \Gamma_s}{e \times \Gamma_s^3} \approx 36 - 100 \gg 1. \quad (2.3)$$

(The range of values is set by the range in  $\Gamma_s$ .) Thus, this quantity is numerically large although it is suppressed by  $\alpha_s^7$  in perturbation theory.

Since this number is greater than one, the jet is surrounded by its own small “fireball” (of size  $\Gamma_s$  or more) where variation of the thermodynamic quantities is very large and hydrodynamics cannot be applicable. Outside of this region, there is a domain where gradients are small enough that viscous hydrodynamics can in principle be used, but the behavior of the fluid is non-linear, dissipative, and possibly turbulent. We will not discuss these complex regions in the present work.

Our current objective is to study what happens far from the jet, where the situation becomes less violent and more tractable. Specifically, it is the region where the flow velocity and pressure modifications may be considered small compared the unperturbed medium, *i.e.* the region where *linearized* hydrodynamics can be used. We note that it is possible to calculate the drag force on an airplane using linearized hydrodynamics, by computing the momentum flow through a large cylinder around the plane. The analogous computation for jets is performed in section V.

In summary one may separate space-time into three regions

1. A region very close to the jet, *i.e.* a region of size  $\Gamma_s$ , where strong dissipative effects happen.
2. A region close to the jet where hydrodynamics is still nonlinear and possibly turbulent.
3. A region far from the jet where the perturbations and gradients are small. In this region one may use linearized hydrodynamics and the motion is laminar.

Since the primordial interaction of the jet with the fluid is complicated and non-linear, we will only study flows in the third linearized region, and impose only general constraints on the total energy, momentum, and entropy deposited by the jet.

### III. LINEARIZED HYDRODYNAMICS IN A STATIC MEDIUM

In this section we will review our results of Ref. [8] where we studied small perturbations of a homogeneous relativistic baryon free fluid at rest. The linearized hydrodynamic equations are written in terms of the small quantities

$$\epsilon = \delta T^{00} , \quad g^i = \delta T^{0i} . \quad (3.1)$$

The remaining components can be expressed in terms of these quantities by means of the equation of state. For a fluid with shear viscosity  $\eta$  and vanishing bulk viscosity these remaining components are

$$T^{ij} = c_s^2 \epsilon \delta^{ij} - \frac{\eta}{w} \langle \partial^i g^j \rangle \quad (3.2)$$

where  $c_s^2 = dp/d\epsilon$  is the speed of sound of the fluid,  $w$  the enthalpy and  $\langle \partial^i g^j \rangle$  is symmetric traceless tensor

$$\langle \partial^i g^j \rangle = \partial^i g^j + \partial^j g^i - \frac{2}{3} \delta^{ij} \partial_i g^i . \quad (3.3)$$

By writing the energy and momentum conservation equations  $\partial_\mu \delta T^{\mu\nu} = 0$ , the linearized hydro equations can be written after a spatial Fourier transforms as

$$\begin{aligned} \partial_t \epsilon + ik g_L &= 0 , \\ \partial_t g_L + ic_s^2 k \epsilon + \frac{4}{3} \frac{\eta}{\epsilon_0 + p_0} k^2 g_L &= 0 , \end{aligned} \quad (3.4)$$

$$\partial_t \mathbf{g}_T + \frac{\eta}{\epsilon_0 + p_0} k^2 \mathbf{g}_T = 0 , \quad (3.5)$$

where  $\mathbf{g} = g_L \frac{\mathbf{k}}{k} + \mathbf{g}_T$ . Thus the equations of linear hydro decouple into two different modes – a sound mode (Eq. (3.4)) and a diffuson mode (Eq. (3.5)). The excitation of these two modes depends on the initial conditions.

In order to study these initial condition, we considered the disturbance produced by an infinitesimal displacement of a particle moving along the  $\hat{x}$  direction with velocity  $\mathbf{v}$  in a time interval  $dt_0$  at time  $t_0$ . According to the axial symmetry of the problem, the most general expression for the initial disturbance is

$$\begin{aligned} \epsilon_{dt_0}(t = t_0, \mathbf{x}) &= e_0(x, r) \\ \mathbf{g}_{dt_0}(t = t_0, \mathbf{x}) &= g_0(x, r) \delta^{ix} + \nabla g_1(x, r) \end{aligned} \quad (3.6)$$

The source functions  $e_0(x, r)$  and  $g_1(x, r)$  excite only the sound mode, while the remaining function  $g_0(x, r)$  excites the diffuson mode. The particular value of these functions depends on the interaction of the jet and the fluid in the near region. As argued in the introduction, it is difficult to find the exact functional form for these sources and they are only constrained by the total energy, momentum, and entropy deposited by the jet.

The hydrodynamic disturbance due to these infinitesimal displacements are calculated as an integral of the sources

$$T^{0\mu}(x) = \int d^3y \left( K_e^\mu(x-y) e_0(y) + K_{g_0}^\mu(x-y) g_0(y) + K_{g_1}^\mu(x-y) g_1(y) \right), \quad (3.7)$$

where the three kernels  $K_e^\mu$ ,  $K_{g_0}^\mu$  and  $K_{g_1}^\mu$  are [8].

$$K_e^\mu = \sum_{i=\pm} \left( \frac{-1}{4\pi r} \partial_r P_i(\Gamma_s), \partial^k \frac{c_s}{4\pi r} i P_i(\Gamma_s) \right), \quad (3.8)$$

$$\begin{aligned} K_{g_0}^\mu = & \sum_{i=\pm} \left( \partial_x \frac{i P_i(\Gamma_s)}{4\pi c_s r}, \partial^k \partial_x \frac{-\int_0^r P_i(\Gamma_s)}{4\pi r} \right) \\ & + \left( 0, \partial^k \partial_x \frac{2 \int_0^r P(\frac{3}{2}\Gamma_s)}{4\pi r} + \delta^{kx} \frac{e^{\frac{-r^2}{2\Gamma_s t}}}{(2\pi \frac{3}{2}\Gamma_s t)^{3/2}} \right), \end{aligned} \quad (3.9)$$

$$K_{g_1}^\mu = \sum_{i=\pm} \left( \frac{i}{4\pi c_s r} \partial_r^2 P_i(\Gamma_s), \partial^k \frac{-1}{4\pi r} \partial_r P_i(\Gamma_s) \right). \quad (3.10)$$

Here we have defined the functions,

$$P_\pm(\Gamma_s) = \frac{1}{\sqrt{2\pi\Gamma_s t}} e^{-\frac{(r\pm c_s t)^2}{2\Gamma_s t}}, \quad P\left(\frac{3}{2}\Gamma_s\right) = \frac{1}{\sqrt{2\pi \frac{3}{2}\Gamma_s t}} e^{-\frac{r^2}{2\frac{3}{2}\Gamma_s t}}. \quad (3.11)$$

In what follows we will try to clarify further the meaning of the different modes as well as their excitations. We will start addressing the problem in the case of inviscid fluid and we will show how to connect to the viscous case. The results presented for dihadron azimuthal distribution will be performed through these solutions.

#### IV. RELATIVISTIC POTENTIAL FLOW

In nonrelativistic laminar flow it is customary to introduce a potential, so that the velocity can be expressed as a gradient,  $\mathbf{v} = \nabla\phi$ . Such flows are clearly irrotational as the  $\nabla \times \mathbf{v}$  vanishes. The conservation of circulation for inviscid fluids guarantees that potential flow remains irrotational throughout the evolution of the liquid. Sound waves, in particular correspond to small potential disturbances over some given flow.

One can define a relativistic analogue of the potential flow for an ideal fluid in which the vorticity of the fluid vanishes [29]. Let us first recall the definition of the vorticity in the relativistic case [30]

$$\omega_{\sigma\tau} = \partial_{[\mu} u_{\nu]} h_\sigma^\mu h_\tau^\nu, \quad (4.1)$$

where  $h^{\mu\nu} = \eta^{\mu\nu} - u^\mu u^\nu$  is the projector into the space perpendicular to the velocity. From this definition, it is simple to see that any flow of the form

$$f u_\mu = \partial_\mu \phi, \quad (4.2)$$

with  $f$  some function, will be irrotational. The scalar field  $\phi$ , called the potential, is the relativistic analogue of the nonrelativistic potential flow.

Thus, one can try to find solutions of the ideal relativistic hydrodynamics of the form Eq. (4.2). In fact, the function  $f$  can be determined by requiring that the projection of the energy momentum conservation equation into the space perpendicular to  $u^\mu$  vanishes,

$$h_{\mu\rho} \partial_\nu T^{\nu\rho} = 0. \quad (4.3)$$

In the case of an ideal baryon free fluid, these equations can be expressed as,

$$s (u^\nu \partial_\nu (T u_\mu) - \partial_\mu T) = 0, \quad (4.4)$$

where  $s$  and  $T$  are the entropy density and temperature of the fluid. It is clear then that, by setting  $f = T$  a velocity field of the form of Eq. (4.2) is a solution of these equations [29]. Thus, imposing irrotationality of the flow leaves us only one equation to solve for the baryon free fluid, the entropy continuity equation.

$$\partial_\mu (s u^\mu) = 0. \quad (4.5)$$

This equation can be used to find a non-linear equation for the potential  $\phi$  (see appendix A 1), which is equivalent to the ideal equations of motion of an irrotational fluid.

Let us conclude by some examples of potential flow. Obviously, the static homogeneous baryon free fluid (which we will use in the rest of the paper) is potential. A slightly less trivial example is the boost invariant Bjorken solution [31]. In appendix A 2 we show how to find this solution from the potential. Finally, as in the nonrelativistic case, sound waves are irrotational disturbances of the hydrodynamic solution and are therefore potential.

### A. Small perturbations of a potential flow

We now will study small perturbations over a given potential hydrodynamic solution. Even though the interaction of the jet with the background fluid leads to very violent flows in the near zone, the small perturbation approximation is always valid far enough away from the high energy particle.

In the region where the perturbation is small, we will have modifications both from the thermodynamic quantities and from the velocity field,  $T'$ ,  $u'_\mu$ .

Let us start with the case where the perturbation of the fluid does not change the irrotational character. In this case, the modified hydrodynamic fields can be described by a perturbation of the potential <sup>2</sup>

$$\phi \rightarrow \phi + \varphi. \quad (4.6)$$

---

<sup>2</sup> Here and in the rest of the paper, the modification of the all the hydrodynamic fields but the potential will be denoted by  $'$ . The modification of the potential denoted by  $\varphi$ .

Expanding the definition of the potential Eq. (4.2) to first order we find

$$\begin{aligned} T' &= u^\mu \partial_\mu \varphi , \\ Tu'_\mu &= h_{\mu\nu} \partial^\nu \varphi , \end{aligned} \tag{4.7}$$

with  $h_{\mu\nu} = \eta^{\mu\nu} - u^\mu u^\nu$ . Note that since  $(u + u')^2 = 1$ , we have  $u \cdot u' = 0$  to first order in the perturbation.

In a general case, since the interaction with the high energy particle is very complicated, the modified field may not be irrotational. However, one can still define a modified potential  $\varphi$  that describes part of the perturbation. In order to do so, we can separate the perturbed velocity field  $u'_\mu = U_\mu + R_\mu$ , such that  $U_\mu$  and  $T'$  are related to the potential  $\varphi$  as in Eq. (4.7). The rotational component  $R$  is then the part of the perturbation that cannot be expressed as Eq. (4.7) and, thus, is linearly independent from  $U$ ; as  $U$  is orthogonal to  $u$ , so is  $R$ .

We now discuss the equations of motion for the perturbations. As we have defined  $U$  such that it can be thought of as coming from a potential, the perturbed transverse equation Eq. (4.3) depends only on  $R$  (and the background quantities)

$$T R^\nu \partial_\nu \partial_\mu \phi + \partial^\nu \phi \partial_\nu (T R_\mu) = 0, \tag{4.8}$$

with  $\phi$  the potential of the background medium. The remaining equation is the the entropy continuity equation for the perturbation

$$\partial_\mu (s u^\mu)' = 0. \tag{4.9}$$

Using the definitions of the speed of sound for a baryon free fluid  $c_s^2 = (s/T) dT/ds$  and the perturbations Eq. (4.7) we can re-express Eq. (4.9) as a second order differential equation for  $\varphi$ :

$$\partial_\mu \left( \frac{s}{T} \left( \eta^{\mu\nu} + \left( \frac{1}{c_s^2} - 1 \right) u^\mu u^\nu \right) \partial_\nu \varphi \right) + \partial_\mu (s R^\mu) = 0. \tag{4.10}$$

Let us mention that such second order differential equation can be expressed as the d'Alambertian of a scalar field in a particular metric [32] that is dependent on the thermodynamic and velocity fields of the background medium:

$$\begin{aligned} \frac{1}{\sqrt{-G}} \partial_\mu \left( \sqrt{-G} G^{\mu\nu} \partial_\nu \phi \right) &= -\frac{1}{\sqrt{-G}} \partial_\mu (s R^\mu) , \\ G^{\mu\nu} &= c_s \frac{T}{s} \left( \eta^{\mu\nu} + \left( \frac{1}{c_s^2} - 1 \right) u^\mu u^\nu \right) , \end{aligned} \tag{4.11}$$

where the rotational component acts as sound source.<sup>3</sup> The reduction of the sound equation to a Klein-Gordon equation in a gravitational background is well known in nonrelativistic fluids where  $G^{\mu\nu}$  is known as the acoustic metric [33].

Let us finally write these general equation for a simple case, the static homogeneous medium. In this case, the equations of motion for the rotational and irrotational field decouple. For the irrotational field, we find the standard wave equation

$$\frac{1}{c_s^2} \partial_t^2 \phi - \nabla^2 \phi = 0. \tag{4.12}$$

---

<sup>3</sup> This emission (that vanishes for the static case) may be important in the final observation of the conical flow

For the rotational mode, we obtain a non propagating equation

$$\partial_0 R_i = 0. \quad (4.13)$$

These two modes coincide with what we called sound and diffuson mode in [8] in the case where the viscosity of the medium  $\eta$  vanishes. As also found there, only the sound mode propagates, while the energy/momentum of the diffuson mode remains localized close to the position of their deposition. Thus, as far away from the source of the perturbation (the jet) the modification of the hydrodynamical fields are small, we expect that only potential flow should be found in this region, since perturbation can only arrive to long distances from the source due to propagation. Thus the irrotational flow should be concentrated in the region close to the jet path. This is also what happens in the case of flow past bodies in nonrelativistic fluids.

## B. Viscosity and Potential Flow

Our previous discussion of the potential flow was made for inviscid fluids only, while now we will study the effect of the shear viscosity. We show below that in the case of static and homogeneous background medium, one can still find a potential solution that describes the system. For non-relativistic fluids this fact has been shown in [34].

The energy momentum tensor for a liquid with non-vanishing shear viscosity is [29]

$$T^{\mu\nu} = w u^\mu u^\nu - \eta^{\mu\nu} p + \eta \langle \nabla^\mu u^\nu \rangle, \quad (4.14)$$

where  $w$  is the enthalpy,  $p$  is the pressure,  $\nabla_\mu = h_{\mu\nu} \partial^\nu$ , and

$$\langle \nabla^\mu u^\nu \rangle = \nabla^\mu u^\nu + \nabla^\nu u^\mu - \frac{2}{3} h^{\mu\nu} \nabla_\mu u^\mu. \quad (4.15)$$

In the case of a viscous fluid, the entropy equation is obtained by projecting  $u^\mu \partial_\nu T^{\mu\nu}$  and leads to

$$\partial_\mu (s u^\mu) = \frac{\eta}{T} \langle \nabla^\mu u^\nu \rangle \partial_\nu u_\mu. \quad (4.16)$$

For a static or homogeneous medium, there is no entropy production due to viscosity. The defining feature of the potential flow is zero vorticity, *i.e.* the existence of solutions of the hydrodynamic equation in the form of Eq. (4.2). For small perturbations on top a static fluid, viscosity will modify the function  $f$  in this equation. As in the inviscid case, the functional form of  $f$  is determined by requiring that the perpendicular hydro equations Eq. (4.3) hold for the viscous case

In order to find  $f$  for the small perturbation, let us expand

$$f = T + f' = T + T' + m \quad (4.17)$$

The first order terms in this expansion coincide with inviscid fluid since viscous corrections vanish for the static homogeneous medium. If there were no viscous corrections,  $f'$  would coincide with the perturbed temperature  $T'$  as in the ideal case. Thus the function  $m$  depends on the viscosity.

Now consider a small perturbation of the hydrodynamic fields,  $T'$  and  $u'^\mu$ . As in the previous section, we can split the velocity perturbation in a potential part that does not have vorticity  $U^\mu$  and a rotational part that carries the vorticity,  $R^\mu$ . We define now a potential related to the irrotational part of the velocity perturbation using Eq. (4.17) as

$$\begin{aligned} T' + m &= u^\mu \partial_\mu \varphi , \\ TU^\mu &= h^{\mu\nu} \partial_\nu \varphi , \end{aligned} \quad (4.18)$$

This definition ensures that if  $R^\mu$  is zero, the perturbed field does not introduce vorticity.

After this identification, the perturbation of the perpendicular equation Eq. (4.3) including shear viscosity can be written in terms of  $R^\mu$  and  $m$  only as

$$\partial_0 R_i + \partial_i m = \frac{3}{4} \Gamma_s \nabla^2 R_i + \Gamma_s \partial_i \nabla^2 \varphi , \quad (4.19)$$

where the right hand side comes from the viscous tensor which has two independent contributions coming from the irrotational and the rotational part of the perturbed velocity field. Thus, identifying

$$m = \Gamma_s \nabla^2 \varphi , \quad (4.20)$$

we absorb all the viscous effects coming from potential flow into a modification of the function  $f$ . After finding this modification due to the viscosity, we can use the definition of the potential Eq. (4.18) into the (perturbed) entropy continuity equation to find an equation for  $\varphi$

$$\partial_0^2 \varphi - c_s^2 \nabla^2 \varphi - \Gamma_s \partial_t \nabla^2 \varphi = 0 . \quad (4.21)$$

The equation for the irrotational part is

$$\partial_0 R_i = \frac{3}{4} \Gamma_s \nabla^2 R_i . \quad (4.22)$$

Eq. (4.21) is the wave equation including dissipation coming from viscosity. This equation for the potential coincides with the equation for the energy density that one would find from our analysis in [8], what is expected as the potential and the energy density in this case are related by a time derivative. Eq. (4.22) is the diffusion equation for the rotational fluid which coincides also with the equation for the diffuson in [8].

## V. ENERGY AND MOMENTUM OF SMALL PERTURBATIONS

As argued in the introduction, an accurate matching of the initial disturbance to the subsequent flow field is not possible. We can only constrain global quantities such as the total energy and momentum deposited. In this section we study the total energy and momentum of the modified fields in order to learn about the possible mechanisms of interaction.

To this end, we consider a very high energy particle that travels with finite velocity  $v$  though an infinite homogeneous ideal baryon free fluid. We also assume that the motion has taken place forever and is therefore static in the rest frame of the particle. The analysis here parallels the discussion of non-relativistic supersonic flow past finite bodies [29].

As shown in section IV A, the equation for small potential perturbations of the potential flow can be readily computed from the acoustic metric, leading to the usual wave equation. We will assume that the potential depends on the combination  $x + vt$ , with  $v$  the velocity of the jet. With this constraint, the wave equation far from the disturbance reads

$$\beta^2 \partial_\kappa^2 \phi - \partial_\perp^2 \phi = 0. \quad (5.1)$$

Here  $\kappa = x + vt$ ,  $\perp$  denotes the coordinates transverse to the jet trajectory, and

$$\beta^2 = \left( \frac{v^2}{c^2} - 1 \right). \quad (5.2)$$

In the region where this equation applies, we can write general solution in the following form:

$$\phi = \frac{T}{2\pi s} \int_{-\infty}^{x+vt-\beta\rho} d\xi \frac{dF/dx(\xi)}{\sqrt{(x+vt-\xi)^2 - \beta^2 \rho^2}}, \quad (5.3)$$

The function  $dF/dx(\xi)$  characterizes the source and will be elucidated in section VI.

From the discussion in section IV A we know that the rotational part of the flow field  $R^\mu$  (in the small perturbation regime) does not propagate and its evolution is determined by the viscosity. Examining the kernel in Eq. 3.9, the rotational field far from the fluid is

$$v^x = \frac{A}{(2\pi \frac{3}{2v} \Gamma_s(x+vt))} \exp \left\{ -\frac{\rho^2}{(\frac{3}{2v} \Gamma_s(x+vt))} \right\}, \quad (5.4)$$

where the constant  $A$  will be determined later<sup>4</sup>. This field also depends on  $x + vt$ .

In order to proceed further, it is beneficial to go to the rest frame of the jet, where the unperturbed medium moves toward the jet with velocity  $v$ . In the jet rest frame, the fields do not depend on the proper time coordinate  $\tau$  and depend only on the longitudinal coordinate<sup>5</sup>.  $\chi = \gamma(x + vt)$ .

The flow picture is sketched in figure 2. The non hydro core co-moving with the jet has a typical transverse size  $\sigma$ . The rotational flow remains concentrated along  $\chi$  to the right of the jet in a narrow wake with a transverse extent that grows as  $\sqrt{\Gamma_s \chi / v \gamma}$ . By contrast, the sonic disturbance propagates and at sufficiently large distances from the jet is concentrated at the Mach angle within a typical size given by  $\sigma$ . Note that for both types of excitations the modified fields are always small sufficiently far away from the jet. The fluid to the left of the jet cannot be modified by the high energy particle and flows with a steady velocity,  $v$ .

In this stationary situation, the energy and momentum loss can be calculated by computing the momentum and energy flux out of a large cylindrical region surrounding the jet. Disregarding the left end cap at  $\chi = -\infty$  (where there is no modification), the surface integral includes the cylinder surface  $C$ , and the right end cap,  $\Sigma$ . The irrotational fluid

<sup>4</sup> The same expression is found in non relativistic fluids past bodies where such field describes the non-turbulent wake behind the body [29]

<sup>5</sup> Note that this conclusion depends on the fact that the velocity of the jet does not change significantly on the passage thought the medium which should be a good approximation for a high energy particle.

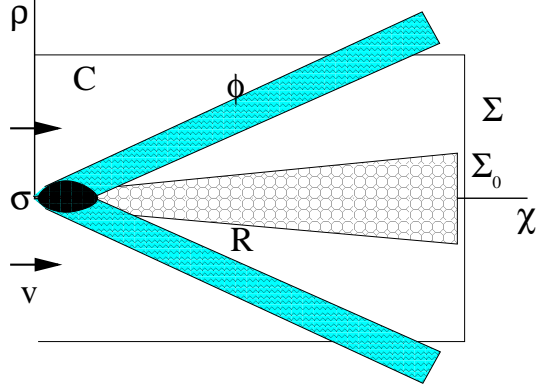


FIG. 2: Sketch of the flow picture in the fluid jet rest frame. The non-hydro core (solid region) serves as a source for the hydrodynamic fields. The irrotational or potential component of the velocity field (wavy region) propagates out of the source and leads to a small disturbance at large distances. The irrotational part (circled region) remains concentrated along the jet axis within a transverse size that grows as  $\sqrt{\chi}$ .

only affects a small subregion  $\Sigma_0$  of the right end cap,  $\Sigma$  of area  $\sim \Gamma_s \chi / v \gamma$ . The potential flow contributes to cylinder  $C$  and to the rest of the end cap,  $\Sigma - \Sigma_0$ . Thus the energy lost by the jet is given by

$$-\frac{dE_j}{d\tau} = \int_C (T^{0\rho})' + \int_{\Sigma - \Sigma_0} (T^{0\chi})' + \int_{\Sigma_0} (T^{0\chi})' \quad (5.5)$$

where ' denotes the variation with respect of the unperturbed field. As in the region  $\Sigma_0$  the main modification of the fields is due to the rotational disturbances, the two first terms in Eq. (5.5) are the energy loss due to the potential flow, while the last is due to the rotational flow, which we denote as  $-dE_j^R/d\tau$ . Since far away from the jet the linear approximation is valid, we have

$$\begin{aligned} (T^{0\rho})' &= (sT\gamma^2 v^\rho)' = T\gamma (s\gamma v^\rho)' + s\gamma v^\rho (T\gamma)' , \\ (T^{0\chi})' &= (sT\gamma^2 v^\chi)' = T\gamma (s\gamma v^\chi)' + s\gamma v^\chi (T\gamma)' . \end{aligned} \quad (5.6)$$

In both these expression we can identify the first term as the modified entropy flux times a constant factor  $(T\gamma)$ . The second term vanishes in the potential region since the fluid is stationary and we have  $(T\gamma)' = \partial_\tau \varphi = 0$ . Next note the entropy produced per unit time is

$$\frac{dS_j}{d\tau} = \int_C (s\gamma v^\rho)' + \int_{\Sigma - \Sigma_0} (s\gamma v^\chi)' + \frac{dS_j^R}{d\tau} \quad (5.7)$$

where  $dS_j^R/d\tau$  is the entropy carried by the rotational flow in the  $\Sigma_0$  region. The two quantities  $dS_j^R/d\tau$  and  $-dE_j^R/d\tau$  are not independent (what we show at the end of the section) but we prefer to keep them explicitly in what is next to make our argument clearer. Putting these results together the energy loss is

$$-\frac{dE_j}{d\tau} = T\gamma \frac{dS_j}{d\tau} - \frac{dE_j^R}{d\tau} - T\gamma \frac{dS_j^R}{d\tau} \quad (5.8)$$

Thus, in the rest frame of the jet, the energy loss of the jet is related to the entropy production minus corrections due to the rotational flow.

Since the high energy particle remains almost on shell as it transverses the medium and loses energy, we conclude that the energy and momentum loss rate are linked by the particle velocity  $v$  as  $dE/dt = vdP/dt$ . In the particle rest frame we conclude that

$$\frac{dE_j}{d\tau} \approx 0. \quad (5.9)$$

This relation immediately allows us to arrive to an important conclusion about the interaction mechanism. From Eq. (5.8) and Eq. (5.9) we conclude that if the interaction mechanism produces significant entropy, then rotational flow is needed and the importance of the rotational flow with respect to the potential flow is related to the contribution of entropy production to the energy loss. Thus, we can distinguish two different types of interactions:

1. Isentropic interactions. The interactions of the jet and the fluid are such that no entropy is produced in the process. In this case the energy/momentum deposited can be calculated from the the far field sonic wave and it is quadratic in the perturbation.
2. Non isentropic interactions. The main mechanism of energy deposition proceeds by transferring of heat into the fluid, creating new entropy. As a consequence, rotational flow is needed, which is concentrated in a narrow wake behind the fluid.

Before continuing we perform a similar analysis for the momentum loss. Integrating over a large cylinder as before, the momentum loss is

$$-\frac{dP_j^\chi}{d\tau} = \int_C (T^{\chi\rho})' + \int_{\Sigma-\Sigma_0} (T^{\chi\chi})' + \int_{\Sigma_0} (T^{\chi\chi})'. \quad (5.10)$$

Now, in the region of small perturbation we find

$$\begin{aligned} (T^{\chi\chi})' &= (v^\chi T^{\chi 0})' = v (T^{\chi 0})' + v^\chi T^{\chi 0} \\ (T^{\chi\rho})' &= (v^\chi T^{\rho 0})' = v (T^{\rho 0})' + v^\chi T^{\rho 0} \end{aligned} \quad (5.11)$$

where we identified a term proportional to the energy loss (due to the potential part of the flow). Denoting,  $d(P_j^\chi)^R/d\tau$  the momentum loss due to the rotational flow (which contains the sum of the momentum flux through the surface  $\Sigma_0$  and  $vdE_j^R/d\tau$ ), the total momentum loss is given by

$$-\frac{dP_j^\chi}{d\tau} = -v \frac{dE_j}{d\tau} + \int_C T s \gamma^2 v^\chi v^\rho + \int_{\Sigma-\Sigma_0} v^\chi T^{0\chi} - \frac{d(P_j^\chi)^R}{d\tau} \quad (5.12)$$

where we separated once again the contributions for the rotational and irrotational part of the flow as in Eq. (5.8). This equation will be useful in the next section.

To complete this section, let us relate the energy and momentum loss and the entropy rate in the wake to the amplitude of the rotatinal field. Boosting Eq. (5.4) to the jet rest frame we find  $v^\chi = v^x/\gamma^2$ , and  $v^\chi$  is a Gaussian in the transverse coordinate  $\rho$  with width depending on  $\chi$ . From Eq. (5.11)

$$-\frac{d(P_j^\chi)^R}{d\tau} = -T s v \gamma^2 \int_{\Sigma_0} v^\chi = -s T v A \quad (5.13)$$

In the same way, by expanding Eq.(5.6) and using the fact that  $dE_j/d\tau = 0$  we obtain

$$\frac{1}{\gamma} \frac{dS_j}{d\tau} = \frac{1}{\gamma} \frac{dS_j^R}{d\tau} + \frac{1}{T\gamma^2} \frac{dE_j^R}{d\tau} = v^2 s A . \quad (5.14)$$

## VI. ISENTROPIC INTERACTIONS

As argued in the previous section, a purely potential excitation of the fluid by a high energy particle implies that no significant entropy can be produced in the interaction. In this case, the perturbed flow field in the far region is given by Eq. (5.3) and depends on a unknown function  $dF/dx(\xi)$  that characterizes the source. To clarify the physical meaning of this source, let  $dF/dx(0)$  mark the smooth beginning of the source which moves with the jet velocity. Further assume that the typical scale of variation of this function  $\lambda$  is much larger than the transverse distance at which Eq. (5.3) is applicable, *i.e.* the source is elongated. In this case, for  $\rho \ll \lambda$  and far away from the tip of the source, we can approximate Eq. (5.3) with

$$\phi = -\frac{T}{2\pi s} dF/dx(x + vt) \ln \left( \frac{\beta\rho}{2(x + vt)} \right) , \quad (6.1)$$

Thus, for transverse distances short compared to the length of the jet, the velocity of the perturbation  $v^\rho$  decreases as  $1/\rho$ , leading to finite radial flux of entropy out of a cylinder close to the jet. With this normalization  $dF/dx(\xi)$  is the entropy flux per unit length at a position  $(\xi)$  with respect to the beginning of the jet. This is completely analogous with the non-relativistic case, where the coefficient is related with the mass flux <sup>6</sup> [29].

As already stated, this analysis is identical to the non-relativistic case of flow past a solid body. As in that case, we see that there is the formation of sound waves, or vorticity free excitation that fall slowly far from the body. This slow fall means that the waves carry energy and momentum out of the body, and we can compute the momentum drag from the far field solution where the linearized approximation is justified. This loss by sonic emission is called sonic drag.

In order to compute the momentum losses and to use standard techniques from text books [29], it is beneficial to go to the rest frame of the jet by performing a Lorentz transformation, as done in the previous section. We will see that in the final expression for the energy and momentum loss all the  $\gamma$  factors drop out, so we can use the expressions obtained for the case of finite mass for massless particles.

As  $\phi$  is a scalar, transforming to the jet rest frame means simply the transformation of the coordinates. Thus, by performing the change of variables  $\xi \rightarrow \xi\gamma$  and defining  $A(\xi) = dF/dx(\xi/\gamma)$ , we obtain

$$\phi = \frac{T}{2\pi s} \int_{-\infty}^{\chi - \bar{\beta}\rho} \frac{A(\xi)}{\sqrt{(\chi - \xi)^2 - \bar{\beta}^2 \rho^2}} d\xi , \quad (6.2)$$

---

<sup>6</sup> In the nonrelativistic case, matter is pushed out of the cylinder by the profile of the solid body that moves in the medium. In our case there is no solid wall which prevents the liquid from reaching center of the jet. However, fluid is pushed out this region by interaction of the medium with the high  $p_T$  particle. We will not speculate further about these microscopic details.

with  $\chi$  the longitudinal coordinate in the jet frame and  $\bar{\beta} = \beta\gamma$ . As we note in the previous section, there is no dependence of the proper time  $\tau$  (stationary situation).

We now express the energy and momentum loss expressions Eq. (5.8) and Eq. (5.12) for the particular case where there is neither entropy production nor rotational flow. In this case the energy loss in the jet rest frame vanishes identically. By using the definition of the perturbed potential,  $Tu'_\mu = \partial_\mu\varphi$  and noting that the perturbed velocity field  $v^\chi$  vanishes as  $\chi \rightarrow \infty$  we conclude that

$$\begin{aligned}\frac{dE_j}{d\tau} &= 0, \\ \frac{dP_j^\chi}{d\tau} &= - \int_C \frac{s}{T} \partial_\chi \phi \partial_\rho \phi,\end{aligned}\quad (6.3)$$

where  $\int_C$  denotes the integral around a cylindrical surface far from the fluid. Eq. (6.3) gives the correct expression of the energy momentum loss by the high  $p_T$  particle if there is neither entropy nor vorticity production.

This is exactly the same expression that is obtained in the nonrelativistic case, but replacing the corresponding quantities as already explained. We can then just refer to standard textbooks [29] to write the final value of the integral.

$$\frac{dP_j^\chi}{d\tau} = -\frac{1}{4\pi} \frac{T}{s} \int_{-L}^L d\xi_1 d\xi_2 \dot{A}(\xi_1) \dot{A}(\xi_2) (\ln |\xi_1 - \xi_2| - \ln(4L)), \quad (6.4)$$

where  $L$  is the longitudinal size of a long cylinder ( $L \gg \lambda$ ) and  $\dot{A}$  denotes the derivative. The last term in Eq. (6.4) diverges in the limit  $L \rightarrow \infty$  unless the flux of entropy out of the cylinder vanish far away from the jet.

We now perform a Lorentz transformation to the fluid frame. We start by noting that according to our definition of  $A(\xi) = dF/dx(\xi/\gamma)$ , we can change the variable of integration in Eq. (6.4) and in the limit  $L \rightarrow \infty$  the expression is independent of  $\gamma$ . The transformation  $dt/d\tau = \gamma$  also cancels the  $\gamma$  factor of the Lorentz transformation leading to an expression for the energy and momentum loss that is applicable when  $v \rightarrow c$

$$\begin{aligned}\frac{dE}{dt} &= -v \frac{dP^\chi}{dt} = -v \frac{dP_j^\chi}{d\tau}, \\ \frac{dP_j^\chi}{d\tau} &= -\frac{1}{4\pi} \frac{T}{s} \int_{-\infty}^{\infty} d\xi_1 d\xi_2 \frac{d}{d\xi} dF/dx(\xi_1) \frac{d}{d\xi} dF/dx(\xi_2) \ln |\xi_1 - \xi_2|. \quad (6.5)\end{aligned}$$

Note that, as a consequence of the first equation in Eq. (6.5), the wave drag is such that the particle remains on shell. The relative sign between the energy and momentum loss is due to the fact that, according to our conventions, the jet is moving in the  $-x$  direction. As the particle remains on shell, the isentropic assumption is a fully consistent way to describe the interaction of the jet and the medium. Note also that we assume that the speed of the propagation did not change, what should not be important for particles moving with velocity close to  $c$ .

## VII. PRODUCTION OF ENTROPY

We discuss now the case where the significant entropy is produced in the interaction of the jet with the medium. In this case the disturbance remains close to the interaction region in

a narrow wake. In the wake, hydrodynamics and linearized hydrodynamics are not justified until the viscosity dissipates the strength of this disturbance. At the end of the section we will also briefly discuss the spectrum of particles produced for such excitations.

In the language of infinitesimal disturbances of section III this case can be accounted for by initial condition such that  $\epsilon_0(t_0, \mathbf{x})$  has a finite integral over space. In the linearized region the total field is found by summing these infinitesimal disturbances. In this setting, it is evident that the energy loss is first order in the perturbation as, to this order, it coincides with the integral of the function  $\epsilon_0$ .

As seen in the section V, the requirement that the particle remains almost on shell on its propagation implies that the production of entropy should be accompanied by vortex flow. In the language of section III it corresponds to a function  $\mathbf{g}_0(t_0, \mathbf{x})$  which cannot be expressed as a gradient ( $\nabla \times \mathbf{v} \neq 0$ ) and with finite integral of the  $\mathbf{g}_0^z$  component. Such a case was studied in [8] with the following particular expressions for the initial conditions:

$$\epsilon_0(t_0, x) = g_0^z(t_0, x) = \frac{dE}{dx} \frac{e^{-(\mathbf{x} - \mathbf{r}_j(t_0))^2/2\sigma^2}}{(2\pi\sigma^2)^3}, \quad (7.1)$$

where  $\mathbf{r}_j(t_0) = (t_0, -t_0, 0, 0)$  is the jet position. In this case, the energy and momentum loss is  $dE/dx$ , and it is first order in the perturbation. Let us note that, as after setting the value of the fields at  $t_0$  we only solve the field equations for  $t > t_0$ , the final solution obtained as the addition of all the disturbances at different times  $t_0$  takes the form

$$T'^{0\nu} = \int dt_0 \theta(t - t_0) \delta T^{0\nu}(t_0), \quad (7.2)$$

where  $\delta T^{0\nu}$  is a solution of the linearized field equations with initial conditions specified at  $t_0$  (section III). Thus, the differential equation that our solution satisfies is, in fact,

$$\partial_\nu T^{\mu\nu} = J^\mu, \quad (7.3)$$

where  $J$  depends on the fields at each  $t_0$  which in the particular case used is

$$J^\mu = \frac{dE}{dx} \frac{e^{-(\mathbf{x} - \mathbf{r}_j(t))^2/2\sigma^2}}{(2\pi\sigma^2)^3} \cdot (1, -1, 0, 0). \quad (7.4)$$

Let us remark here that the source Eq. (7.3) used in [8] is the same used in [22] to solve hydrodynamic equations in the nonlinear regime in an expanding, boost invariant, ideal, baryon free fluid<sup>7</sup>. Thus, our solution is the linearized version of this problem for a homogeneous medium.

After reexpressing the fields in this way, we want to connect the description of the fluid in terms of section IV and show that excitations where entropy is produced the modification of the fields are mainly concentrated in the near region. This is clearly seen from the rotational component (excited by  $g_{t_0}^z$ ). As demonstrated in section IV A, for a static medium the vorticity of the fluid does not propagate, and the disturbance remains close to the deposition region, *i.e.* in a region of typical size  $\sigma$  the source size, and thus far from the source size the

---

<sup>7</sup> the actual calculation in [22] integrates several of these sources along the space rapidity  $\eta$  in order to keep boost invariance but the conclusions should not change

fluid is potential. This was also found in [8] by solving the equations of motions including viscosity.

Thus, if the interaction jet liquid is such that significant total entropy is produced, then the modification of the hydro fields are mainly produced in the near region (the ‘non-hydrodynamic core) and, as argued in the introduction, they should not be described in terms of ideal hydrodynamics; one instead would need to use dissipative hydro in order to gain some understanding from this region.

To conclude this section let us briefly discuss the particle production for medium excitations that produced entropy, which will be extensively done in the next section for the entropy free case. As found in [8], the excitation of the diffusion mode (vorticity) leads to matter moving preferentially in the direction of the jet. This flow is due to the region close (distances of the order of  $\sigma$ ) to the jet path and leads to a complete shadowing of any Mach cone signal in the dihadron azimuthal distributions, resulting in correlations only at  $\Delta\phi = \pi$ . Similar conclusions have been reached in [22], confirming our result for the linearized static theory in the non linear expanding regime. Thus, this kind of excitations, if present, leads to a fill up of the Mach cone in the two particle correlations associated to the jet. For more details we refer the reader to our short paper [8] and to [22]. Let us remark once again that our calculated spectrum in [8] is dominated by the near region, where the non hydrodynamic core is, and thus, the description in terms of hydrodynamics is not justified.

## VIII. SPECTRA AND CORRELATIONS ASSOCIATED WITH THE JET

We now calculate the spectrum of particles associated with a jet through the induced disturbance of the medium. We will consider, as in the previous discussion, a jet propagating in a static homogeneous baryon free fluid. The jet is created at some time  $t_0 = 0$  and is absorbed due to the energy loss at some later time  $t_j$ . We take the life time of the jet  $t_j$  as a parameter, which means that, for a fixed value of the energy loss, we are varying the energy of the jet. In a realistic simulation, this time would be given by the energy loss and the spectrum of produced jets. Finally, the system freezes out at a time  $t_f$  where we calculate the spectrum though the Cooper Fry prescription [35]. We will always consider  $t_j < t_f$  so that the final spectrum is not dominated by our arbitrary source.

We will only study the case where there is no entropy production, and consequently the energy loss is second order. We will consider the superposition of infinitesimal disturbances described in section III and demand that no entropy is produced. This can be achieved by considering infinitesimal displacements such that the modification of the fields at a time  $t_0$  in a time interval  $dt_0$  is

$$\begin{aligned} \epsilon_{dt_0} &= 0 , \\ g_{dt_0}^i &= \frac{C}{\sigma^4} \partial_i e^{-r^2/2\sigma^2} . \end{aligned} \tag{8.1}$$

The source size  $\sigma$  is the characteristic distance from the jet such that the linearized approximation is valid. The amplitude of the disturbance is  $C/\sigma^4$  with  $C$  a dimensionless constant. The factor  $1/\sigma^4$  is introduced *ad hoc* such that the disturbances have the correct dimensions keeping  $C$  dimensionless.

As explained in the introduction, the process by which the energy of the jet is thermalized is highly dissipative and we cannot describe it. Thus, we cannot fix from first principles the

two parameters of the initial perturbation  $C$  and  $\sigma$  unless a good matching mechanism is found. Thus we will use the energy and momentum loss to relate their values. Following appendix B we can relate this disturbance with a far field solution in the form Eq. (5.3). After appendix B, we identify the function  $dF/dx$  in term of the parameters  $C$  and  $\sigma$  as

$$\frac{dF}{dx}(\xi) = -\frac{2\pi v^2}{T} \frac{C}{c_s^3 \bar{\sigma}^2} \partial_\xi e^{-\xi^2/2\bar{\sigma}^2}, \quad (8.2)$$

where we have introduced for simplicity  $\bar{\sigma} = v\sigma/c_s$ . With this identification we can evaluate the energy loss using Eq. (6.5) leading to

$$\frac{dE}{dt} \approx \frac{\pi^2}{v} \frac{1}{sT} \frac{C^2}{\sigma^6}. \quad (8.3)$$

As expected, the energy loss is quadratic in the amplitude of the disturbance,  $C$ . The strong dependence on the typical size  $\sigma$  is partly artificial and comes from our choice of using  $\sigma$  as the dimensionfull parameter while keeping  $C$  dimensionless.

We will also consider that the static medium has a non vanishing shear viscosity that leads to a reduction of the amplitude of the sound waves as it propagates out of the disturbance. As this attenuation of the wave can be understood [29] as a result of the dissipation of the mechanical energy (given by Eq. (8.3)), we will use the previous formula for the energy/moment loss also in the viscous case.

Let us summarize here the parameters that we have in our calculation. The source has two parameters, the amplitude  $C$  and the source size  $\sigma$ . This two can be constrained by the value of the energy loss. The timings are characterized by the jet lifetime  $t_j$  and the observation time  $t_f$ . In a realistic simulation, the lifetime is determined from the jet energy and energy loss; the freeze out, time from the hydrodynamical simulations at RHIC. Finally, the medium is characterized by the speed of sound  $c_s$ , the sound attenuation length  $\Gamma_s$  and the temperature of the static medium. We will fix the speed of sound to be  $c_s = 1/\sqrt{3}$  and we will not consider its change here in spite of our findings in [25] that showed that those changes are very important for the final observation and the position of the peaks. The value of  $\Gamma_s$  is taken close to its minimal bound  $\Gamma_s = 1/4\pi T$  [28]. Finally, everything is calculated in units of the temperature, that should be of the order of the critical temperature. From now on we will assume that the jet moves at the speed of light  $v = 1$ . Let us finally give a numerical value by substituting the QGP equation of state as measured by lattice calculation [27] ( $e \approx 12T^4$ )

$$\frac{dE}{dt} \approx 0.63 \frac{C^2}{\sigma^8} \sigma^2 \frac{1}{T^4}. \quad (8.4)$$

Once we have listed all the parameters that enter in our calculation we can calculate the spectrum of particles induced by the jet. As the medium is static, we use as the Cooper Fry prescription for equal time freeze out surface as in [8]

$$\frac{dN}{d^3p} = \int_V \frac{d^3V}{2\pi^3} e^{-\frac{E}{T} + \delta}, \quad (8.5)$$

where  $V$  is the volume of the fireball,  $T$  is the temperature at freeze out and  $\delta$  the perturbation of the fluid. For  $\delta = 0$  we obtain the unperturbed spectrum from the static medium. When a jet goes through the fluid,  $\delta$  is related to the modified fields as:

$$\delta = \frac{E}{T} \frac{\delta T}{T} + \frac{\vec{p}\vec{v}}{T}. \quad (8.6)$$

From these expression we expect non trivial features of the  $p_T$  dependence of the correlation function. As discussed in [8], we can distinguish two different regimes in the particle production:

1. Low energy particles  $E \sim T$ . In this region we can expand the exponential in Eq. (8.5) and express the spectrum in terms of the energy and momentum deposited

$$\frac{dN}{d^3p} = \frac{e^{-\frac{E}{T}}}{(2\pi)^3} \left( V + \frac{E}{T} \frac{E_{dep}}{w} + \frac{\vec{P}}{T} \frac{\vec{P}_{dep}}{w} \right). \quad (8.7)$$

The term proportional to the fireball volume  $V$  corresponds to the uncorrelated contribution that is subtracted from the dihadron correlation function. The other two terms are due to the disturbances. As seen in Eq. (8.7), the soft particles are insensitive to the particular shape of the flow field and the angular dependence is just a cosine of the relative angle between the observed particle and the jet. Thus, linearized hydrodynamics is unable to produce peaks for very soft particles.

2. High energy particles  $E \gg T$ . In this region the large parameter  $E/T$  compensates the small flow velocity. The integral is then dominated by the maximum of the exponent. Thus, the final spectrum reflects the shape of the sonic disturbance and only points of maximum modification of the hydrodynamic fields contribute to the integral. This fact is also responsible for the absence of the conical flow when significant entropy is produced. In this case the region of maximum modification is close to the jet and the spectrum is dominated by the near field region where the applicability of the hydrodynamic approach is uncertain.

Finally, we calculate the spectrum of correlated particles by subtracting the unperturbed spectrum ( $\delta = 0$ ) from the jet induced spectrum ( $\delta \neq 0$ )

$$\frac{dN}{dyd\phi} = \frac{dN}{dyd\phi} \Bigg|_{\delta \neq 0} - \frac{dN}{dyd\phi} \Bigg|_{\delta=0}. \quad (8.8)$$

### A. Comparison with experimental data

From the previous discussion of the spectrum we expect that for sufficiently large energy particles, the azimuthal distribution of particles associated with the jet should reflect the modification of the flow fields due to the particle passage. As argued in [8] this translates into the appearance of large angle correlations in the azimuthal dihadron distribution associated with the jet. Such large angle correlations have been observed by both the PHENIX [14] and STAR [15] collaborations.

In this section we will fix a set of values for our parameters that give similar dihadron correlation than those in [14] with no other justification as to reproduce qualitative features of observed on experiment. Those values are  $\sigma = 0.75/T$ ,  $\Gamma_s = 0.1/T$ ,  $dE/dx = 6.3T^2$ ,  $t_j = 8/T$  and  $t_f = 10/T$ . The corresponding correlations functions are shown in the lower left panel of figure 3. Let us note that for a typical temperature of the plasma of the order of  $T \approx 200$  MeV, the required value of the energy loss is very large  $dE/dx = 12.6$  GeV/fm. If we however would use a more realistic value of the energy loss  $dE/dx = 2$  GeV/fm we

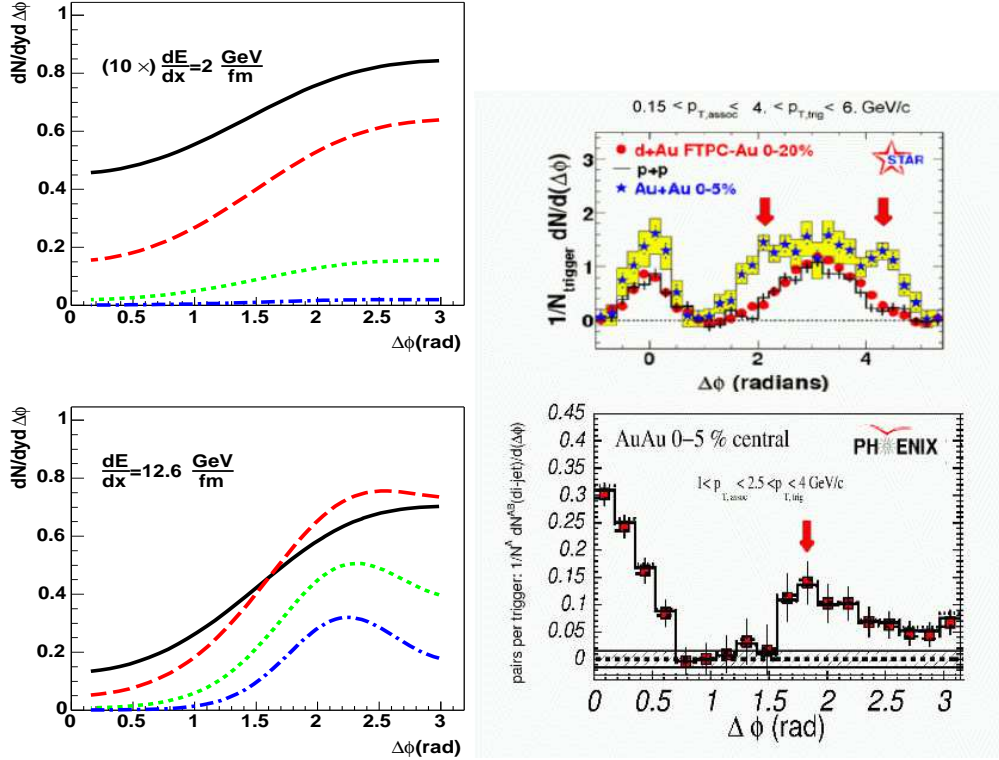


FIG. 3: Left: Associate yield dependence on associate  $p_T$  for fixed source size  $\sigma = 0.75/T$ , viscosity  $\Gamma_s = 0.1/T$ ,  $t_j = 8/T$ ,  $t_f = 10/T$ , and energy loss,  $dE/dx = 10T^2$  (top) and  $dE/dx = 63T^2$  (bottom). The label values for  $dE/dx$  correspond to  $T = 200$  MeV. The three curves are for  $1T < p_t < 5T$  (solid),  $5T < p_t < 10T$  (dotted),  $(3\times) 10T < p_t < 15T$  (dashed),  $(10\times) 15T < p_t < 20T$  (dashed-dotted). (in the upper panel all the curves are rescaled further up by a factor 10). No large angle correlation is observed for  $dE/dx = 10T^2$ . For  $dE/dx = 63T^2$  the position of the peak shifts toward  $\pi$  for lower  $p_T$ . Right: Experimental dihadron azimuthal distributions from STAR (top) [15] and PHENIX (bottom) [14]

are not able to generate any large angle correlation or magnitude of the correlation for the intervals of momentum considered, as shown in the upper left panel of figure 3.<sup>8</sup>

Even though the necessary value of the energy loss within our static approximation is very large, we will try to argue in the next section, where we discuss the dependence of the calculated spectrum on the different parameters, that expansion effects may help to reduce the necessary energy loss. That is why we want to point out here some qualitative agreement of our calculation (with large energy loss) with the experimental data. This is the  $p_T$ -dependence of the correlation.

In the lower left panel of figure 3 ( $dE/dx = 12.6$  GeV/fm) we show the  $p_T$  dependence of the azimuthal dihadron correlation for different  $p_T$  windows. The four curves correspond to  $p_T$  intervals (in units of temperature) of 1-5, 5-10, 10-15, 15-20 for solid, dotted, dashed and

<sup>8</sup> Let us note however that, according to [36] RHIC data seem to support values of  $\hat{q}$  that are up to 4 times larger than those of the perturbative estimates from [26], which lead to energy losses that are much closer to our required value.

dashed dotted respectively. Note that we have rescaled up the two highest  $p_T$  bins by factors 3 and 10 respectively. This figure shows clearly the behavior of the correlation function. As claimed, at low  $p_T$ , when the ratio  $p_T/T$  is small (solid line), the formation of conical flow in the Mach direction is not reflected in particle spectra; we obtain, in fact, that particles are produced mainly in the direction opposite to the jet. As  $p_T$  increases, the correlation develops, moving the peak to the left toward the Mach angle and making the width of the peak at this angle smaller. In the upper left panel, for smaller values of  $dE/dx$  (where all the curves are further rescale up by 10), the correlation always peaks at  $\Delta\phi = \pi$  for the intervals of  $p_T$  considered. This is because the fields in this case are too weak.

In figure 3 (right panel) we show the dihadron correlation function as presented by STAR (top) [15] and PHENIX (boton) [14]. Even though our calculation cannot be directly compared to the experimental situation, as we have not included the effect of the expansion [20, 21] nor the variable speed of sound [25], that may be very important for the final observation of the effect, some qualitative features seem to be reproduced. In fact, the correlation function shown by STAR, seems to be a broad peak with a small peak at a finite angle away from  $\pi$  (marked by the red arrows). This could be explained from our discussion of the  $p_T$  dependence as in the experimental conditions of STAR, where the associated  $p_T$  is dominated by soft particles ( $0.15 < p_T < 4 \text{ GeV}/c$ ), and thus, according to the previous discussion, the strength of the correlation should be small, as is due to the high-pt tail of the associated particles. On the contrary, in the case of PHENIX, where the associated particles are harder ( $1 < p_T < 2.5 \text{ GeV}/c$ ), the correlation function shows a well defined peak off  $\pi$ . What is more, for the particular values of the parameters chosen, the amplitude of our calculated correlation function corresponds roughly with the experimental magnitude observed.

Let us remark here that the  $p_T$  dependence of the correlations coming from the conical flow, which seems to be in agreement with the experimental situation, is completely different from those radiative based mechanism to explain large angle correlation [17, 18, 19]. These model predict that the correlations should shift toward  $\Delta\phi = \pi$  as the  $p_T$  of the associated particle increases, which is the opposite to what we find.

The position of the peak in our correlation function is at  $\Delta\phi \approx \pi - \arccos(1/\sqrt{3}) = 2.2 \text{ rad.}$  and is set by the value of the speed of sound in the medium, which in our case is the ideal QGP value of  $c_s^2 = 1/3$ . This is of course not the case in the experimental condition at RHIC, where as the medium expands and cools, the speed of sound changes from the previous QGP value to  $c_s^2 \approx 0$  in the mixed phase and  $c_h^2 \approx 0.2$  in the hadron gas. From hydrodynamical simulations of Au-Au collisions at RHIC leads to similar (proper) time extension of the three previously mentioned phases of approximately  $\tau \sim 4 - 5 \text{ fm}$ . As argued in [8] the Mach angle depends only on the ratio of distance traveled by the disturbances to the one traveled by the jet; thus the position of the peak is modified due to the expansion and can be estimated from the average speed of sound along the evolution of the medium

$$\cos \theta_M = \frac{1}{c\tau} \int_0^\tau c_s dt \approx 0.333 \implies \Delta\phi \approx \pi - 1.2 \text{ rad.} , \quad (8.9)$$

This value agrees nicely with the experimental value shown in the experimental correlation function as seen in figure 3 b)

Finally, in figure 4 we show the spectrum of correlated particles in the away side jet. We defined the away side as particles as  $\Delta\phi > 1$  as in [15]. We compare it with the spectrum

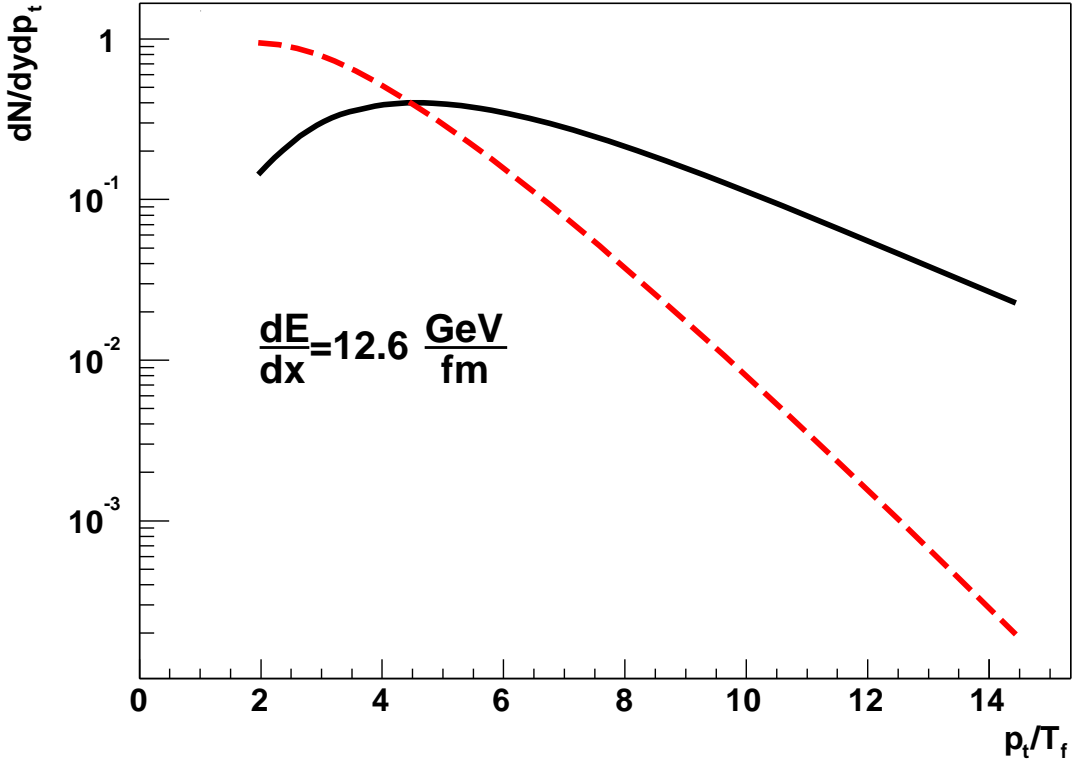


FIG. 4: Spectrum of associated particles in the away side  $\Delta\phi > 1$  for  $\sigma = 0.75/T$ ,  $dE/dx = 142T^2$ ,  $\Gamma_s = 0.1/T$  (solid). Spectrum of uncorrelated particles (rescaled down by a factor 100). The associated yield is much harder than the inclusive due to the boosted liquid induced by the jet.

obtained for uncorrelated particles, as if no jet were produced. In order to be able to show both in the same plot, we rescale down this last spectrum (that we will call inclusive) by a factor hundred. We observe that the correlated spectrum is harder than the inclusive one. This is due to the fact that the liquid is boosted due to the non zero velocity fields in the Mach direction. The experimental spectrum shown in [15] also seems slightly harder than the inclusive one, however the effect is by no means so prominent. On the other hand our inclusive spectrum is much steeper than those in [15] as our background fluid lacks radial flow. Thus, even though there is no quantitative agreement between our calculation and STAR data in this issue, it could be due to the static approximation that we took for the liquid, that is definitely not true.

## B. Dependence on the parameters

In the previous subsection we saw that in order to produce similar correlation functions as the experimental ones we need too large values for the energy loss. In this section we want to show that our calculation is very sensitive to the parameters chosen.

In figure 5 we study the dependence on the energy loss (or the source amplitude) for the rest of the parameters fixed. We vary the energy loss by a factor of two from the central value of  $dE/dx = 63T^2$  (*i.e.* 25.2, 12.6, 6.3 GeV/fm for  $T = 200$  MeV). We observe an extremely strong dependence on the amplitude (note that the solid curved is rescaled down

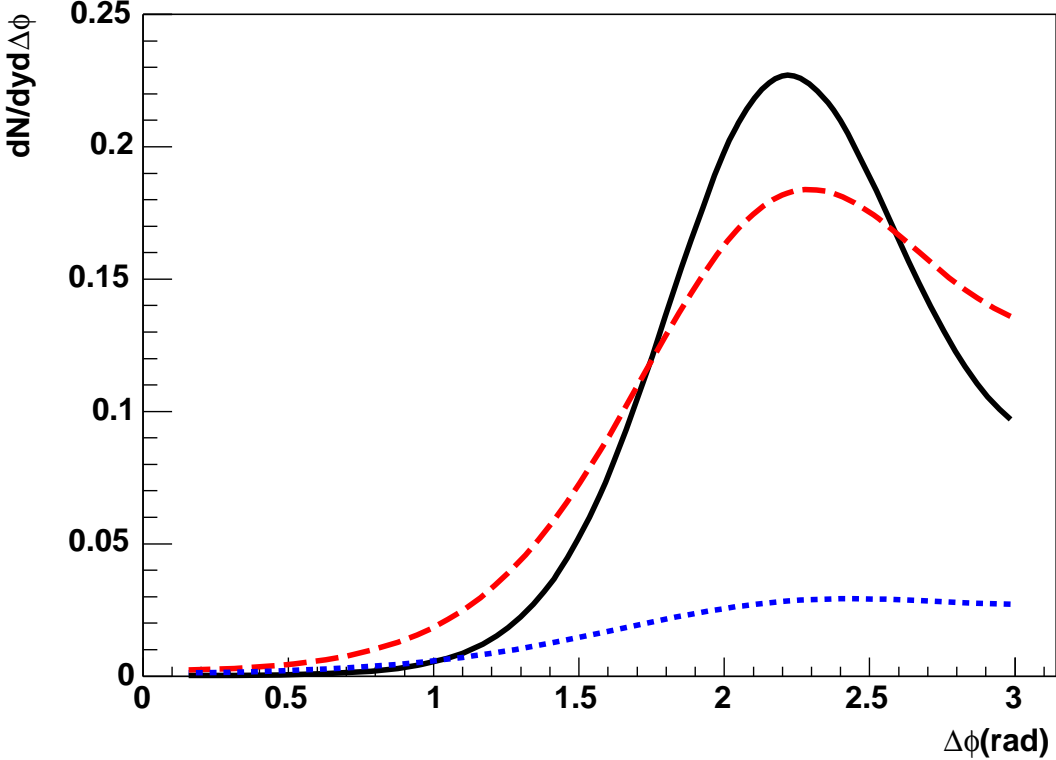


FIG. 5: Associate yield dependence on energy loss for fixed source size  $\sigma = 0.75/T$ ,  $\Gamma_s = 0.1/T$ ,  $t_j = 8/T$ ,  $t_f = 10/T$  and  $10T < p_t < 20T$ . The three curves are for  $(1/20 \times) dE/dx = 126T^2$ ,  $dE/dx = 63T^2$ ,  $dE/dx = 35.5T^2$  for solid, dotted and dashed respectively.

by a factor 20). This is easily understood as from Eq. (8.5) we see that the amplitude enters in the exponent and thus small changes lead to large variations on the final observation. This strong dependence is the basis for our claim that expansion effects may be very important for the final observation of the effect on experimental conditions as it can reduce the needed values of  $dE/dx$ .

In [25] two of us found, by studying a simple model for a dynamic medium (that of a static fluid in an expanding universe), that the expansion of the liquid and dropping of the speed of sound leads to an enhancement of the ratio  $v/T$ . Estimates made for RHIC tell us that for disturbances originated at early times, such enhancement can be as big as a factor 3. What this means for the spectrum is that at the time of freeze out, the amplitude of the disturbance can be up to a factor 3 smaller than in the static case to reproduce the same correlation (as the smaller amplitude is compensated by the dropping density and speed of sound of the background medium). Such a smaller value of the amplitude enters quadratically into the energy density what means that the energy loss can be up to a factor 9 smaller than those showed in the static case.

In figure 6 we study the source size dependence of the number of associated particles to the jet  $dN/dy d\Delta\phi$  in an interval of transverse momentum  $10T_f < p_T < 20T_f$  for the mid rapidity region  $y=0$  for fixed values of the energy loss ( $dE/dx = 63T^2$ ) and the jet energy ( $t_j = 8/T$ ) at a freeze out time of  $t_f = 10/T$ . We observe that the smaller the source size the smaller the signal in the azimuthal dihadron correlations. This dependence is due mainly to the viscosity. When the source size is comparable to the sound attenuation length, viscous

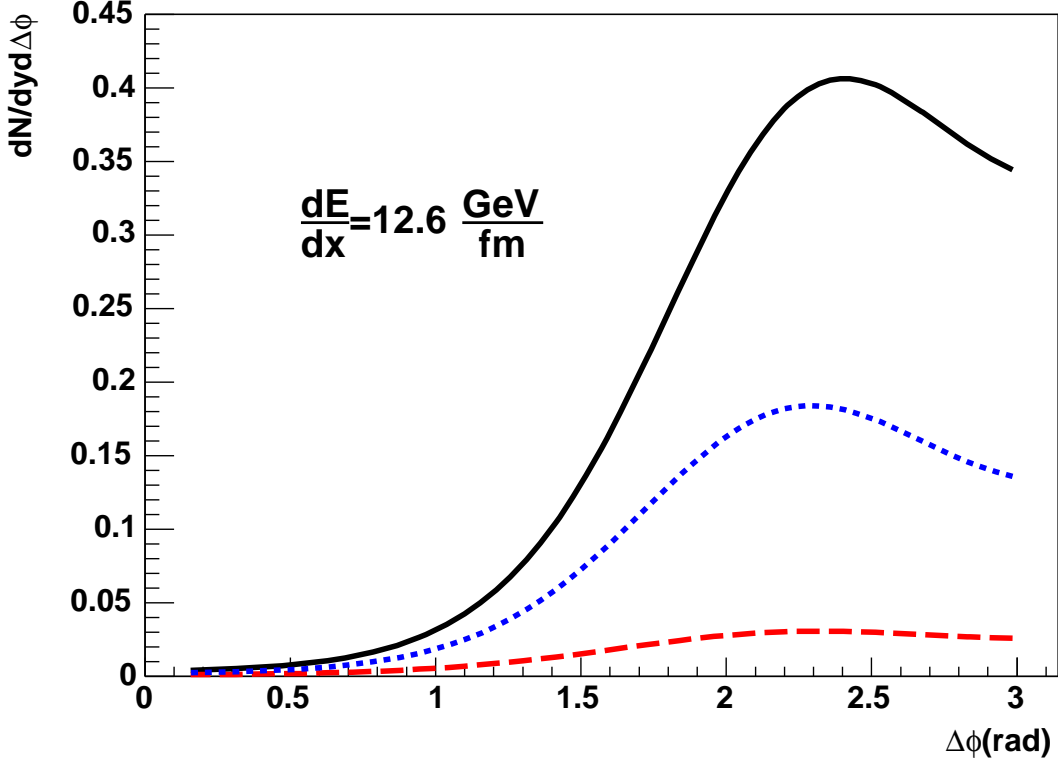


FIG. 6: Associate yield dependence on source size  $\sigma$ , for fixed energy loss  $dE/dx = 63T^2$ ,  $\Gamma_s = 0.1/T$ ,  $t_j = 8/T$ ,  $t_f = 10/T$  and  $10T < p_t < 20T$ . The three curves are for  $\sigma = 1/T$ ,  $\sigma = 0.75/T$  and  $\sigma = 0.5/T$  for solid, dashed and dotted respectively.

effects reduce the amplitude very fast. For larger sources, the reduction of the amplitude is delayed till times of the order of

$$t_r \approx \sigma^2/\Gamma_s . \quad (8.10)$$

We also notice that as the size grows, the peak in the correlation shifts slightly toward  $\pi$ . This is because the interference of sound waves leads to the Mach angle for propagation and observation times larger than the typical size of the object (as an extreme example consider a large object that moves an infinitesimal distance at supersonic velocity; it is clear then that it only can generate spherical waves).

In figure 7 we show the dependence on the sound attenuation length  $\Gamma_s$  for  $\sigma = 0.75/T$  and  $dE/dx = 63T^2$  for three different values of the viscosity  $T$   $\Gamma_s = 0.1, 0.2, 0.5$  for solid, dotted and dashed lines respectively (note that the two last ones are rescaled up by a factor 10 and 20 respectively). As in the case of the amplitude, the correlation function is very sensitive to the value of the viscosity. By changing the viscosity by a factor of 2 the whole correlation structure almost disappears and gets reduced by an order of magnitude. Increasing the viscosity by a factor 5 leads to hardly no signal in the dihadron azimuthal distribution. This is because the dissipative effects induce a reduction of the amplitude of the fields.

In figure 8 we study the dependence on the energy of the jet though the jet life time for a fixed energy loss. We also fixed the source size  $\sigma$  and the viscosity  $\Gamma_s$ . We again observe a strong dependence of the correlation strength on the energy of the jet. This is in a sense

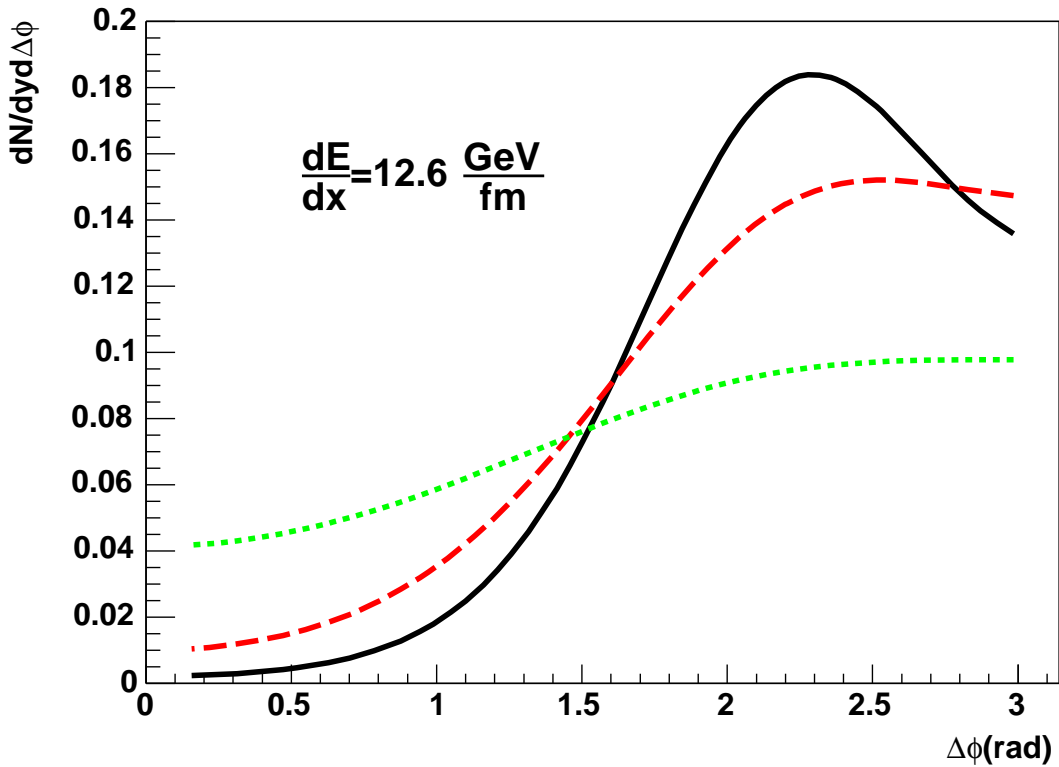


FIG. 7: Associate yield dependence on viscosity for fixed source size  $\sigma = 0.75/T$  and energy loss,  $dE/dx = 63T^2$ ,  $t_j = 8/T$ ,  $t_f = 10/T$  and  $10T < p_t < 20T$ . The three curves are for  $\Gamma_s = 0.1/T$ ,  $(5\times) \Gamma_s = 0.2/T$ ,  $(20\times) \Gamma_s = 0.5/T$  for solid, dotted and dashed respectively

due to the dependence on the viscosity. As the jet has less energy it gets absorbed earlier in the medium and thus the sonic disturbances have to propagate longer before freeze out. Thus, the attenuation of the waves leads to very strong suppression of the correlation signal. The strong dependence on the path length complicates the interpretation of the large angle correlations due to the conical flow, as it seems to filter out a tight range of jet energies, reducing the total amplitude. However this dependence on the path may not be directly extrapolate to the real expanding case, as in such situation, the energy loss and the viscosity will depend on time. Thus, even though longer times are required to observe a particle that is absorbed earlier, the large values of the amplitude and the smaller value of the viscosity at early times leads to an enhancement on the final observation. Thus, detailed studies in a real case should be performed before conclusions on the path length dependence.

By the previous studies of the different parameters we want to show that the appearance of conical flow seems to be very fragile, given the large changes observed in the correlation for small changes of the different characteristic scales lead to completely different correlation strengths and shapes. However, if the interpretation of the large angle correlation as coming from conical flow survives further tests, this strong dependence reveal that this prove seems to be very sensitive to the details of the dissipative processes in the medium. This strong dependence leads us to have some hope to use this prove in order to learn about the transport properties on the medium. The situation is however unfortunate at the moment due to the freedom we have in the parameters. If we could constrain the source size by some microscopic model, the energy loss would constrain the amplitude of the wave, leaving us with a very

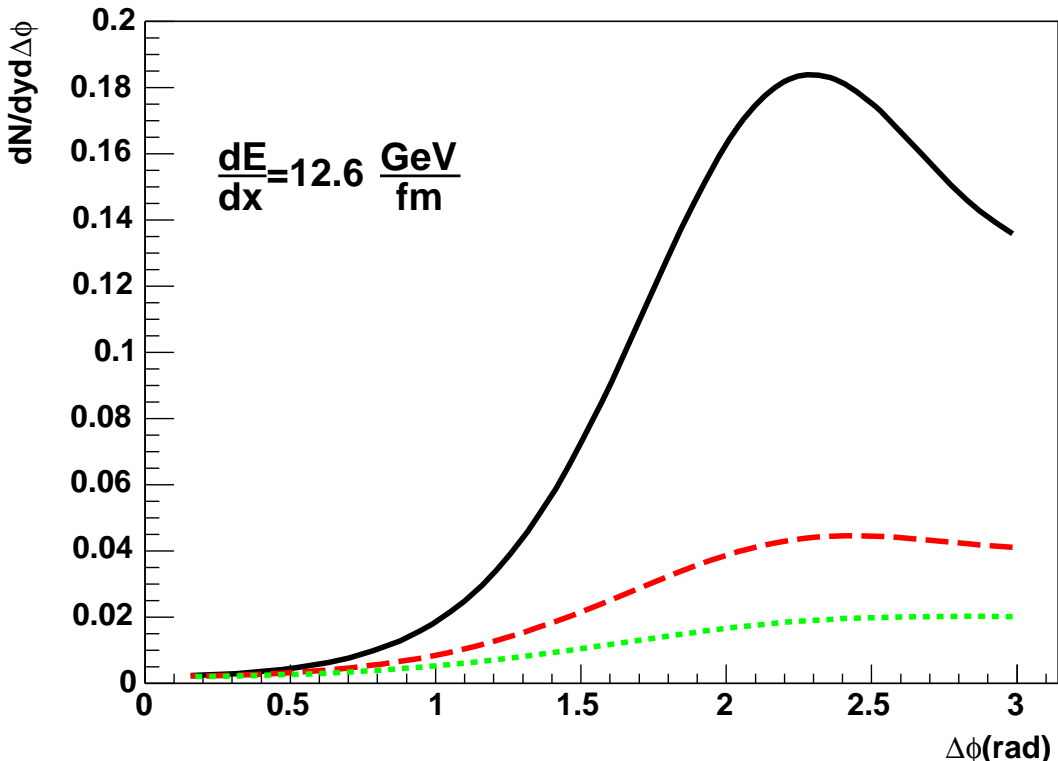


FIG. 8: Associate yield dependence on the jet life time  $t_j$  for fixed source size  $\sigma = 0.75/T$  energy loss,  $dE/dx = 63T^2$ , viscosity  $\Gamma_s = 0.1/T$ ,  $t_j = 8/T$ ,  $t_f = 10/T$  and  $10T < p_t < 20T$ . The three curves are for  $t_j = 8/T$ ,  $t_j = 7/T$ ,  $t_j = 6/T$ , for solid, dotted and dashed respectively

sensitive prove of the viscosity. Unfortunately such constraints are not available at the moment.

## IX. CONCLUSIONS

In this paper we have extended our studies in Ref. [8] of the linearized hydrodynamic equations which describe the interaction of jets with quark gluon plasma. We have clarified the origin of the two hydrodynamic modes that we called sound and diffuson in Ref. [8] and related them to vortex free and rotational solutions.

We then used the relativistic analogue potential flow to find the governing equations of these modes in an expanding background. For a static background, we subsequently used these equations to systematically study the interaction of a jet with the medium. Generally the jet can excite both the sound and the diffusion modes. The entropy produced by the jet-medium interaction fixes the strength of the diffusion mode relative to the sound mode. This entropy is localized in a narrow wake along the direction of the jet.

The equations for the sound wave are given by Eqs. (4.2), and (5.3). The unknown function in this formula,  $dF/dx$ , is related to the momentum transferred to the sound wave – see Eq. (6.5). Similarly the flow fields in the wake are given by Eq. (5.4), and the amplitude  $A$  in this formula is fixed by the momentum transferred to the wake – see Eq. (5.13). This momentum transfer is in turn related by Eq. (5.14) to the total entropy produced by the

jet. In summary, by specifying the total rate of energy loss and entropy production the flow fields at large distances are determined.

Regardless of the mechanism of excitation, a supersonic jet in a static fluid leads to flow at the Mach angle. However, the different mechanisms of excitation may or may not lead to visible peaks in the final particle spectra. If the jet-medium interaction produces significant entropy, the wake contribution obscures the Mach angle in the final spectrum. Only very strong jet-medium interaction which does not produce significant entropy can yield hydrodynamic fields that give peaks in the azimuthal correlation functions at the Mach angle,  $\Delta\phi \approx \pi - 1.2$  rad. For example, for an isentropic jet-medium interaction with a large energy loss  $dE/dx \approx 12$  GeV/fm in a static medium, the resulting flow produces azimuthal distributions of the same order of magnitude as those observed by PHENIX and STAR [14, 15]. Unfortunately, for moderate energy loss,  $dE/dx = 2$  GeV/fm, the flow is unable to qualitatively reproduce the data. However, we argued previously that the expansion may amplify the sound wave and ultimately reduce the required  $dE/dx$  [25]. We have also shown that for the large  $dE/dx$ , the  $p_T$  dependence of the correlation function has some of the qualitative features of the experimental measurements.

If the jet-medium interaction does not produce significant entropy, the observation of peaks in the angular distribution is possible, but it is very sensitive to the characteristic scales involved. Systematic study of the viscosity, the jet-medium interaction time, the freeze out time, and the source size  $\sigma$ , reveals that the prediction of a Mach cone from linearized hydrodynamics is quite fragile and depends on many of the microscopic details of the interaction of the jet with the medium. Further work is needed to clarify these microscopic details before a strong conclusion can be reached.

**Acknowledgments.** This work was partially supported by the Department of Energy (U.S.A.) under grants DE-FG02-88ER40388 and DE-FG03-97ER4014.

---

- [1] K. Adcox *et al.* (PHENIX), *Phys. Rev. Lett.* **88** (2002) 022301
- C. Adler *et al.* (STAR), *Phys. Rev. Lett.* **89** (2002) 202301
- S. S. Adler *et al.* (PHENIX), *Phys. Rev. Lett.* **91** (2003) 072301
- J. Adams *et al.* (STAR), *Phys. Rev. Lett.* **91** (2003) 172302
- [2] J. D. Bjorken, FERMILAB-PUB-82-059-THY
- [3] X. N. Wang, M. Gyulassy and M. Plumer, *Phys. Rev. D* **51** (1995) 3436  
    M. Gyulassy, I. Vitev, X. N. Wang and B. W. Zhang, arXiv:nucl-th/0302077.
- [4] A. Kovner and U. A. Wiedemann, arXiv:hep-ph/0304151.
- [5] R. Baier, Y. L. Dokshitzer, A. H. Mueller, S. Peigne and D. Schiff, *Nucl. Phys. B* **483** (1997) 291  
    R. Baier, Y. L. Dokshitzer, A. H. Mueller and D. Schiff, *JHEP* **0109** (2001) 033
- [6] E. V. Shuryak and I. Zahed arXiv:hep-ph/0406100
- [7] Wang X N, 2004 [arXiv:nucl-th/0405017]
- [8] J. Casalderrey-Solana, E. V. Shuryak and D. Teaney, *J. Phys. Conf. Ser.* **27** (2005) 22, [arXiv:hep-ph/0411315]
- [9] H. Stoecker, [arXiv:nucl-th/0406018]
- [10] E. Shuryak, *Prog. Part. Nucl. Phys.* **53** (2004) 273 [arXiv:hep-ph/0312227].

- [11] G. Baym, H. Monien, C. J. Pethick and D. G. Ravenhall, Phys. Rev. Lett. **64** (1990) 1867.
- [12] P. Arnold, G. D. Moore and L. G. Yaffe, JHEP **0305**, 051 (2003) [arXiv:hep-ph/0302165].
- [13] D. Teaney, *Phys. Rev. C* **68** (2003) 034913
- [14] S. S. Adler *et al.* (PHENIX Collaboration), [arXiv:nucl-ex/0507004]
- [15] J. Adams *et al.* (STAR Collaboration), *Phys. Rev. Lett.* **95** (2005) 152301
- [16] J. Ruppert and B. Muller, *Phys. Lett.* **B** 618 123,2005
- [17] I. M. Dremin, [arXiv:hep-ph/0507167]
- [18] V. Koch, A. Majumder, X. N. Wang, [arXiv:nucl-th/0507063]
- [19] I. Vitev, [arXiv:hep-ph/0501255]
- [20] L. M. Satarov, H. Stoecker, I. N. Mishustin, *Phys. Lett.* **B** 627 64,2005
- [21] T. Renk, J. Ruppert, [arXiv:hep-ph/0509036]
- [22] A. K. Chaudhuri and U. Heinz, [arXiv:nucl-th/0503028]
- [23] G. L. Ma *et al.*, [arXiv:nucl-th/0601012]
- [24] Z. W. Lin *et al.*, *Phys. Rev. C* **72** (2005) 064901
- [25] J. Casalderrey-Solana, E. V. Shuryak, [arXiv:hep-ph/0511263]
- [26] R. Baier, *Nucl. Phys. A* **715** (2003) 209
- [27] F. Karsch, *Lect. Notes Phys.* **583** (2002) 209
- [28] G. Policastro, D. T. Son and A. O. Starinete, *Phys. Rev. Lett.* **87** (2001) 081601
- [29] L. D. Landau and E. M. Lifshitz, *Fluid Mechanics*
- [30] A. H. Taub, *Ann. Rev. Fluid. Mech.* **10** (1978) 301
- [31] J. D. Bjorken, *Phys. Rev. D* **27** (1983) 140
- [32] N. Bilic, [arXiv:gr-qc/9908002]
- [33] C. Barcelo, S. Liberati, M. Visser, [arXiv:gr-qc/0505065]
- [34] D. D. Joseph, *J. Fluid. Mech.* **479** (2003) 191
- [35] F. Cooper and G. Frye, *Phys. Rev. D* **27** 140.
- [36] K. J. Eskola, H. Honkanen, C. A. Salgado, U. A. Wiedemann, *Nucl. Phys. A* **747** (2005) 511

## APPENDIX A: ABOUT THE EQUATIONS OF THE POTENTIAL

### 1. Derivation of the dynamic equation

In this section we derive a nonlinear equation for the potential introduced in section 4. As in the case of irrotational flow for ideal hydrodynamics, the only non trivial equation is the entropy continuity equation Eq. (4.5) the equation for the potential arises from re expressing Eq. (4.5) in terms of  $\phi$ . Let us start by writing Eq. (4.5) as

$$\partial_\mu \frac{s}{T} \partial^\mu \phi + \frac{s}{T} \partial_\mu \partial^\mu \phi = 0 . \quad (\text{A1})$$

As for a baryon free fluid the speed of sound can be expressed as

$$c_s^2 = \frac{s}{T} \frac{dT}{ds} , \quad (\text{A2})$$

we can express the first derivative on Eq. (A1) in terms of derivatives of the temperature as

$$\partial_\mu \frac{s}{T} = \frac{s}{T} \left( \frac{1}{c_s^2} - 1 \right) \frac{1}{2T^2} \partial_\mu T^2 . \quad (\text{A3})$$

Now we note that from the definition of  $\phi$  we obtain

$$T^2 = \partial_\mu \partial^\mu \phi . \quad (\text{A4})$$

Dropping the factor  $s/T$  and multiplying by  $T^2$ , we obtain the following nonlinear equation equation for  $\phi$

$$\left( \frac{1}{c_s^2} - 1 \right) \partial_\mu \phi \partial_\nu \phi \partial^\mu \partial^\nu \phi + \partial_\mu \phi \partial^\mu \phi \partial_\nu \partial^\nu \phi = 0 . \quad (\text{A5})$$

For a baryon free fluid, the hydrodynamic equation reduces to the energy momentum conservation. Thus, in the case where the initial conditions for ideal hydrodynamics do not introduce any vorticity, the equation derived is totally equivalent to solving the standard system of equation of conservation of the stress energy tensor.

### 2. Bjorken solution as potential flow.

As an example of potential flow let us look for a boost invariant solution of hydrodynamics with no transverse expansion [31]. We will assume that the initial conditions do not introduce any vorticity, and thus, all the properties of the flow field can be derived from a potential  $\phi$ . As  $\phi$  is a scalar, the requirement of boost invariance imposes that  $\phi$  is a function of the proper time  $\tau = \sqrt{t^2 - z^2}$  only. For this potential, the nonlinear differential equation Eq. (A5) takes the form

$$\left( \frac{d}{d\tau} \phi \right)^2 \left( \frac{1}{c_s^2} \frac{d^2}{d\tau^2} \phi - \frac{1}{\tau} \frac{d}{d\tau} \phi \right) = 0 . \quad (\text{A6})$$

Using the relation between the temperature and the potential Eq. (A4) we obtain  $T$  as a function of  $\tau$

$$T = \frac{d}{d\tau} \phi(\tau) . \quad (\text{A7})$$

Thus, Eq. (A6) becomes a first order equation for the temperature

$$\frac{d}{d\tau} T + \frac{c_s^2}{\tau} T = 0 , \quad (\text{A8})$$

which, by means of the equation of state leads to

$$\frac{1}{s} \frac{d}{d\tau} s + \frac{1}{\tau} = 0 , \quad (\text{A9})$$

the solution of which is  $s \propto 1/\tau$ , the well known Bjorken solutions [31]. The velocity field can also be readily calculated from the potential. From its definition,  $T u_\mu = \partial_\mu \phi$ , we obtain that the velocity field is  $u^\tau = 1$  or

$$u^\mu = \frac{1}{\tau} (t, 0, 0, z) , \quad (\text{A10})$$

that coincides again with the result due to Bjorken [31].

## APPENDIX B: FAR FIELD FROM SUMMING INFINITESIMAL DISTURBANCES

We now want to connect our previous solution on [8] with our general expression Eq. (5.3) for the perturbed fields in the ideal case. The goal is to show that both ways of calculating give the same expression in the region far from the fluid. However, extra terms from those in Eq. (5.3) appear that are only significant in the region close to the jet.

As argued along the text, the potential flow describes sound waves, that are also described for the system of equations Eq. (3.4). Setting  $\eta = 0$ , the system of equations can be written as the wave equation for  $\epsilon$ . We will consider the solution for an infinitesimal disturbance that happens in a time interval  $dt_0$  around  $t_0$  that leads spherically symmetric disturbance

$$\epsilon_{dt_0}(t_0, \mathbf{x}) = e_0(\mathbf{R}_{t_0}) , \quad (\text{B1})$$

$$g_{dt_0}(t_0, \mathbf{x}) = g_0(\mathbf{R}_{t_0}) , \quad (\text{B2})$$

where  $\mathbf{R}_{t_0} = \sqrt{(x + t_0)^2 + \rho^2}$  for a jet moving at the speed of light along the  $-x$  direction. The total disturbance is obtained by the addition of all the infinitesimal disturbances.

The general solution for the spherically symmetric wave takes the form

$$\epsilon_{t_0} = \frac{1}{R_{t_0}} (f_- (R_{t_0} - c_s(t - t_0)) + f_+ (R_{t_0} + c_s(t - t_0))) \quad (\text{B3})$$

The values of the two functions are set by the initial condition Eq. (B1) at  $t_0$ . As the incoming wave  $f_+$  is only important in the region of the order of the source size we can neglect it in the far field.

From the definition of the potential in the static case, the perturbed temperature can be as  $T' = \partial_t \varphi$  and thus, by means of the equation of state, we obtain the potential

$$\varphi_{dt0} = \frac{1}{R_{t_0}} (F(R_{t_0} - c_s(t - t_0))) , \quad (B4)$$

where  $\dot{F} = c_s^2 f_- / s$  where  $\dot{F}$  denotes time derivative. The addition of all the infinitesimal disturbances leads to

$$\varphi = \int_{-\infty}^{\infty} dt_0 \theta(t - t_0) \frac{F(R_{t_0} - c_s(t - t_0))}{R_{t_0}} . \quad (B5)$$

The solution Eq. (B5) can be rewritten as Eq. (5.3) by introducing a  $\delta$ -function as

$$F(R_{t_0} - c_s^2(t - t_0)) = \int_{-\infty}^{\infty} d\xi \frac{c_s}{v} F\left(-\frac{c_s}{v}\xi\right) \delta(R_{t_0} - c_s(t - \xi/v - t_0)) \quad (B6)$$

The integration of over  $t_0$  can be done now by solving the delta function. This is standard and after this solution, we can express

$$\frac{\delta(R_{t_0} - c_s(t - \xi/v - t_0))}{R_{dt0}} = \frac{\delta(t_0 - t_i)}{c_s((x + vt - \xi)^2 - \beta^2 \rho^2)^{1/2}} \quad (B7)$$

with  $\beta$  defined in Eq. (5.2), and  $t_i$  is the solution of the  $\delta$ -function.

$$t_i - t + \frac{\xi}{v} = \frac{v}{v^2 - c_s^2} \left( - (x + vt - \xi) \pm \sqrt{(x + vt - \xi)^2 - \beta^2 \rho^2} \right) . \quad (B8)$$

The existence of solutions for the  $\delta$ -function imposes a constraint in the  $\xi$  integration such that the radicand in Eq. (B8) is greater than zero. The  $\theta$ -function in Eq. (B5) constraints further this integration. Imposing  $t > t_i$  leads to two different integration regions:

1.  $x + vt > c_s^2/v^2(x + vt - \beta\rho)$ , that includes the region inside of the Mach cone. In this case requiring that  $t > t_0$  leads to the field

$$\varphi = \frac{1}{v} \left( 2 \int_{-\infty}^{x+vt-\beta\rho} d\xi - \int_{-\infty}^{-vR_t/c} d\xi \right) \frac{F\left(-\frac{c_s}{v}\xi\right)}{((x + vt - \xi)^2 - \beta^2 \rho^2)^{1/2}} \quad (B9)$$

2.  $x + vt < c_s^2/v^2(x + vt - \beta\rho)$ , that corresponds to the field out of the cone. The field is then

$$\varphi = \frac{1}{v} \int_{-\infty}^{-vR_t/c} d\xi \frac{F\left(-\frac{c_s}{v}\xi\right)}{((x + vt - \xi)^2 - \beta^2 \rho^2)^{1/2}} \quad (B10)$$